REGULAR ARTICLE

blood advances

Late fetal hematopoietic failure results from ZBTB11 deficiency despite abundant HSC specification

Huimin Cao,[1,2] Shalin H. Naik,[3-5] Daniela Amann-Zalcenstein,[4-6] Peter Hickey,[4-6] Agus Salim,[7,8] Benjamin Cao,[1,2] Susan K. Nilsson,[1,2,*] M. Cristina Keightley,[1,9,10,*] and Graham J. Lieschke[1,*]

[1]Australian Regenerative Medicine Institute, Monash University, Clayton, VIC, Australia; [2]Biomedical Manufacturing, Commonwealth Scientific and Industrial Research Organisation, Clayton, VIC, Australia; [3]Department of Immunology and [4]Single Cell Open Research Endeavour, The Walter and Eliza Hall Institute of Medical Research, Parkville, VIC, Australia; [5]Department of Medical Biology, University of Melbourne, Parkville, VIC, Australia; [6]Advanced Genomics Facility, Advanced Technology and Biology Division, The Walter and Eliza Hall Institute of Medical Research, Parkville, VIC, Australia; [7]Mathematics and Statistics, La Trobe University, Bundoora, VIC, Australia; [8]Melbourne School of Population and Global Health, School of Mathematics and Statistics, University of Melbourne, Parkville, VIC, Australia; [9]La Trobe Institute for Molecular Science, La Trobe University, Bundoora, VIC, Australia; and [10]Rural Clinical Sciences, La Trobe Rural Health School, Bendigo, VIC, Australia

Key Points

- Zbtb11 is crucial for HSC function in establishing and maintaining early murine hematopoiesis.
- Absence of Zbtb11 in the hematopoietic compartment leads to dysregulation of niche and oxidative phosphorylation genes.

Hematopoiesis produces diverse blood cell lineages to meet the basal needs and sudden demands of injury or infection. A rapid response to such challenges requires the expansion of specific lineages and a prompt return to balanced steady-state levels, necessitating tightly coordinated regulation. Previously we identified a requirement for the zinc finger and broad complex, tramtrak, bric-a-brac domain–containing 11 (ZBTB11) transcription factor in definitive hematopoiesis using a forward genetic screen for zebrafish myeloid mutants. To understand its relevance to mammalian systems, we extended these studies to mice. When *Zbtb11* was deleted in the hematopoietic compartment, embryos died at embryonic day (E) 18.5 with hematopoietic failure. *Zbtb11* hematopoietic knockout ($Zbtb11^{hKO}$) hematopoietic stem cells (HSCs) were overabundantly specified from E14.5 to E17.5 compared with those in controls. Overspecification was accompanied by loss of stemness, inability to differentiate into committed progenitors and mature lineages in the fetal liver, failure to seed fetal bone marrow, and total hematopoietic failure. The $Zbtb11^{hKO}$ HSCs did not proliferate in vitro and were constrained in cell cycle progression, demonstrating the cell-intrinsic role of Zbtb11 in proliferation and cell cycle regulation in mammalian HSCs. Single-cell RNA sequencing analysis identified that Zbtb11-deficient HSCs were underrepresented in an erythroid-primed subpopulation and showed downregulation of oxidative phosphorylation pathways and dysregulation of genes associated with the hematopoietic niche. We identified a cell-intrinsic requirement for Zbtb11-mediated gene regulatory networks in sustaining a pool of maturation-capable HSCs and progenitor cells.

Submitted 19 December 2022; accepted 18 July 2023; prepublished online on *Blood Advances* First Edition 11 August 2023. https://doi.org/10.1182/bloodadvances.2022009580.

*S.K.N., M.C.K., and G.J.L. contributed equally to this study.

The scRNA-seq mouse HSC data have been deposited in the Gene Expression Omnibus database (accession number GSE240459).

RNAseq data of WT and zbtb11-deficient zebrafish neutrophils have been deposited in the Gene Expression Omnibus database (accession number GSE239949).

The authors declare that all remaining data supporting the findings of this study are available within the article and its supplemental Files, or on request from the corresponding authors, Graham J. Lieschke (graham.lieschke@monash.edu) and Cristina Keightley (c.keightley@latrobe.edu.au).

The full-text version of this article contains a data supplement.

Introduction

Hematopoietic stem cells (HSCs) are characterized by the dual hallmarks of stemness: producing daughter HSCs (self-renewal) and/or daughter progenitor cells (differentiation).[1-4] Progenitors proliferate and differentiate in response to specific signals that engender different blood lineages.[2] Under steady-state hematopoiesis, adult HSCs can remain dormant for long periods before responding to the growth/differentiation stimuli. In contrast, developing HSCs emerge from the embryonic aorta, proliferate to seed hematopoietic niches, and generate a balanced hematopoietic output before exiting the cell cycle and awaiting a stimulus for reentry.[5] HSCs have limited capacity for continued cell cycling and eventually succumb to replicative stress, resulting in exhaustion.[5] All of these processes are tightly regulated by the measured interplay between cytokines, growth factors, adhesion molecules, and transcription factors.[6,7]

ZBTB11 (zinc finger and broad complex, tramtrak, bric-a-brac [BTB] domain–containing protein 11), originally identified as a repressor of metallothionein 2A,[8] is a member of the ZBTB superfamily of transcription factors. These proteins regulate crucial biological processes, including proliferation, morphogenesis, apoptosis, protein degradation,[9,10] and hematopoiesis.[11-17] We previously showed that ZBTB11 is required for cell cycle progression in zebrafish,[18] suggesting its potential involvement in oncogenesis.[19] ZBTB11 also plays an emerging role in response to viruses.[20-22] Clinically, *ZBTB11* mutations have recently been associated with intellectual disability,[23-26] and interest in ZBTB11 function is burgeoning, with multifaceted roles emerging recently.[27-29]

A key role for Zbtb11 as a hematopoietic regulator was first identified in the zebrafish *zbtb11*-deficient mutant marsanne.[18] In marsanne, all blood lineages, including HSCs, are initially formed, but after switching to HSC-dependent hematopoiesis, multilineage development fails, accompanied by the loss of HSCs.[18] This suggests an essential role for Zbtb11 in HSC maintenance and continued HSC longevity; however, it is not known whether this function is conserved in mammals. To assess the role of Zbtb11 in mammalian hematopoiesis and HSC maintenance, we generated *Zbtb11*$^{fl/fl}$ mice crossed with *vav-iCre*[30] to delete *Zbtb11* from the hematopoietic compartment (*Zbtb11*^{hKO}). In *Zbtb11*^{hKO} mice, HSCs are specified in abundance yet do not generate adequate numbers of lineage-committed progenitors or mature differentiated blood cells, leading to hematopoietic failure and death by E18.5. Investigation of Zbtb11 target genes led us to identify novel Zbtb11-mediated gene regulatory axes that are pivotal for balancing hematopoietic output.

Materials and methods

Animals

Vav-iCre (B6.Cg-Tg[Vav1-iCre]A2Kio/J) mice (The Jackson Laboratory, Bar Harbor, ME)[31] were crossed with blue fluorescent protein (BFP) mice, and both sexes were bred at the Monash Animal Research Platform (Monash University, Clayton, VIC, Australia) using standard husbandry practices. Enhanced flippase (FLPe)-deleter mice were purchased from and crossed at the Monash Animal Research Platform. Experiments were performed according to the protocols approved by the relevant animal ethics and institute biosafety committees.

Zbtb11^{hKO} mouse

Zbtb11^{hKO} mice were generated in-house at the Gene Recombineering and Monash Gene Technology Facility. Targeting constructs were generated (supplemental Figure 1A), and 2 verified targeted clones were used to generate germ line-transmitting knockout lines by pronuclear injection into C57BL/6J blastocysts, according to standard protocols.[32] Before analysis, the neomycin selection cassette was removed by crossing with a ubiquitous FLPe-deleter mouse line and mice with an excised neocassette were crossed as vav-iCre × BFP. Because no phenotypic difference was observed between heterozygotes and wild-type (WT), these were included together in the WT/control groups.

Flow cytometry

Timed matings and isolation of the fetal liver (FL), bone marrow (BM), spleen, and long bones have been described previously.[33] FL or BM cells were immunolabeled with a lineage cocktail (anti-B220, anti-CD3, and anti-Gr1), anti–Sca-1, anti–c-Kit, anti-CD48, anti-CD150, anti-CD127, anti–Fms-like receptor tyrosine kinase 3 (anti-Flt3), anti-CD34, and anti-CD16/32 antibodies. Cells were analyzed as hematopoietic stem and progenitor cells (Lin$^-$Sca-1$^+$c-Kit$^+$ [LSK]), HSC (Lin$^-$Sca-1$^+$c-Kit$^+$CD150$^+$CD48$^-$), myeloerythroid progenitors (Lin$^-$CD127$^-$Sca-1$^-$c-Kit$^+$CD34$^-$CD16/32$^-$), granulocyte–macrophage progenitors (Lin$^-$CD127$^-$Sca-1$^-$c-Kit$^+$CD34$^+$CD16/32$^+$), common myeloid progenitors (CMPs; Lin$^-$CD127$^-$Sca-1$^-$cKit$^+$CD34$^+$CD16/32$^-$), common lymphoid progenitors (Lin$^-$CD127$^+$Sca-1$^+$c-Kit$^+$Flt3$^+$), lymphoid-primed multipotent progenitors (LSKCD34$^+$Flt3$^+$), differentiated myeloid cells (Gr1/Mac-1$^+$), and differentiated lymphoid cells (B220$^+$ and CD3$^+$). Flow cytometry was performed using an LSRII flow cytometer (BD Biosciences) as previously described.[34] To assess the cell cycle, 1 to 2 ×10^6 FL cells were immunolabeled with an anti-Gr1 lineage cocktail and anti–Sca-1/-c-Kit, antibodies, washed, and then stained with anti-Ki67-BV786 (BD Biosciences) and Hoechst 33342 (20 μg/mL) using Fixation/Permeabilization Kit (Thermo Fisher Scientific) according to manufacturer's instructions.

Transplantation homing assay

Sorted E16.5 FL HSC were labeled with the fluorescent tracking dye carboxy fluorescein diacetate succinimidyl ester (5(6)-carboxyfluorescein diacetate N-succinimidyl ester when incorporated; Molecular Probes, Eugene OR) for *Zbtb11*^{hKO} and semi-naphtorhodafluor-1-acetoxymethylester (Invitrogen) for controls to use as donor cells, as previously described.[34] Briefly, a total of 4000 to 8000 donor cells were transplanted into each nonirradiated WT neonate recipient via intraperitoneal injection with an additional nonablated 200 000 whole-BM carrier cells. Transplanted cell numbers were standardized as follows: twice as many control vs *Zbtb11*^{hKO} HSCs were injected to account for the doubling of FL HSC in *Zbtb11*^{hKO} mice compared with that in controls. Homing efficiency of transplanted donor HSCs was assessed after 15.5 hours.[34] Independent experiments were performed using cells from pooled *Zbtb11*^{hKO} pups each time.

BM sections

E17.5 femurs were dissected,[33] embedded in Tissue-Tek Optimal Cutting Temperature compound (ProSciTech), and sectioned on a cryostat. Sections were fixed and stained with hematoxylin and

eosin, and slides were scanned using an Olympus dotSlide microscope to reconstruct a complete image.

Single-cell RNA sequencing

A total of 186 single E14.5 FL *Zbtb11*^{hKO} and control HSCs were assayed on one 384-well plate using an adapted version of the CelSeq 2 protocol.[35,36] Paired-end sequencing was performed on Illumina NextSeq500 with the following run parameters: read1 = 14nt, read2 = 78nt, and phiX = 2%. Expression was quantified by counting the number of unique molecular identifiers mapped to each gene using scPipe (https://www.bioconductor.org/packages/scPipe, Bioconductor). Cells were evenly split between the WT and *Zbtb11*^{hKO} (n = 93 each). Cell cycle classification was implemented using the cyclone function of the scran R/Bioconductor package. The expression values were normalized and denoised using the scran::denoisePCA function. The output of preprocessing identified 181 cells and 15 069 genes. Seurat was used to perform unsupervised clustering. Clusters corresponding to cell types were identified using the Louvain algorithm in Seurat. Differential expression analyses were performed to ascertain marker genes in each cluster. Marker genes were used to find the top 10 gene ontology (GO) and Kyoto encyclopedia of genes and genomes (KEGG) pathways in each cluster. Cluster-independent differential expression analysis was performed between samples using glmFit from edgeR to compare WT and *Zbtb11*^{hKO} cells while blocking the estimated cell cycle phase (expanded in supplemental Methods).

RNAseq

Our RNA sequencing (RNAseq) data set comparing differential gene expression between *zbtb11*^{C116S} and WT neutrophils was generated as previously described.[18] It was remined using zebrafishmine.org (AllianceMine, https://www.alliancegenome.org) GO enrichment for genes dysregulated in *zbtb11*^{C116S} neutrophils compared with those in WT neutrophils, with a false discovery rate < 0.05.

Statistics

Descriptive and analytical statistics were calculated using Prism 9 (GraphPad Software Inc). Unless otherwise stated, the data were obtained from ≥3 experiments. The details are included in the figure legends.

Results

Homozygous deletion of Zbtb11 results in defective FL hematopoiesis

We previously identified Zbtb11 as a transcriptional repressor required for hematopoiesis in zebrafish.[18] To determine whether this role is conserved in mammals, *Zbtb11*$^{fl/fl}$ mice were generated and mated with *Vav1-iCre* × *BFP* to disrupt *Zbtb11* in the hematopoietic compartment (supplemental Figure 1A). Genomic polymerase chain reaction confirmed the deletion of 976 bp spanning exon 2 of Zbtb11 (supplemental Figure 1B). No *Zbtb11*$^{fl/fl}$ *vav-iCre*$^{+}$ (*Zbtb11*^{hKO}) mice were born (supplemental Figure 1C), and timed mating determined that the absence of Zbtb11 in the hematopoietic compartment resulted in acute lethality by E18.5. From E14.5 to E16.5, gross morphology was largely unaffected in *Zbtb11*^{hKO} embryos, and the weight remained normal. At E17.5 and E18.5, however, *Zbtb11*^{hKO} embryos showed significant growth retardation (supplemental Figure 1D,F). Homozygous *Zbtb11*^{hKO} embryos were immediately distinguishable from heterozygous or *Zbtb11*-replete siblings based on their pallor from at least E14.5 onwards, indicating severe anemia (supplemental Figure 1F). A schematic description of the analysis is provided in Figure 1A. Despite no differences in embryo weight up to E16.5, FL cellularity significantly decreased from E14.5 to E17.5 in *Zbtb11*^{hKO} vs in controls (Figure 1I; supplemental Figure 1E). At E16.5 and E17.5, there were significantly fewer *Zbtb11*^{hKO} FL CD45^{+} leukocytes (Figure 1B,D). By E17.5, both lymphoid and myeloid lineages were dramatically depleted in the *Zbtb11*^{hKO} (Figure 1C,E-G). For all *Zbtb11*^{hKO} populations, the cell number did not significantly increase from E16.5 to E17.5, whereas a robust increase occurred in controls (Figure 1D-G), denoting severely compromised differentiation and/or proliferation potential in FL in the absence of Zbtb11.

With such a strong phenotype in homozygous hematopoietic knockouts, we examined whether there was a *Zbtb11* haploinsufficiency phenotype in heterozygotes. No significant difference between the homozygous WT and *Zbtb11* heterozygous embryo weight or FL cellularity was apparent (Figure 1H-I). Likewise, across mature lineages, committed progenitors, and multipotent progenitors, cell numbers from embryos heterozygous for the *Zbtb11*^{hKO} allele were not significantly different from those of WT in the FL or BM (supplemental Figures 2A-K and 3A-K). This demonstrated that hematopoietic compromise resulting from *Zbtb11* loss in this model required disruption of both *Zbtb11* alleles.

Zbtb11 is required for the generation of committed hematopoietic progenitors during fetal development

We analyzed the number of lineage-committed progenitors in FL to assess whether Zbtb11 loss preferentially affected the differentiation of specific lineages (Figure 2A). At E14.5, there was no difference in the number of lineage-committed progenitors between *Zbtb11*^{hKO} and controls (Figure 2E-G,I). In contrast, at E16.5 and E17.5, *Zbtb11*^{hKO} lymphoid-primed multipotent progenitors, CMPs, granulocyte-monocyte progenitors, myeloerythroid progenitors, and common lymphoid progenitors were all significantly decreased compared with controls (Figure 2B-I). Although all progenitor types significantly increased between E16.5 and E17.5 in controls, there was no increase in *Zbtb11*^{hKO} progenitors, and CMP progenitor numbers even decreased between E14.5 and E17.5, respectively ($P = .030$). This is concordant with the reduction in mature differentiated lineages (Figure 1B-I) and is consistent with the requirement for Zbtb11 to support the size of the progenitor cell compartments from which mature cell types are derived by proliferation and differentiation.

Zbtb11-deficient multipotent progenitors and phenotypic HSCs accumulate in the FL during development

Reduced *Zbtb11*^{hKO} lineage-committed progenitors and mature cells could result from disruption of homeostasis in the HSC compartment. Therefore, we investigated the number of *Zbtb11*^{hKO} stem cells and multipotent progenitors using flow cytometry (Figure 3A). Surprisingly, and in contrast to committed progenitors and mature cells, there was more than double the number of *Zbtb11*^{hKO} LSK multipotent progenitors at E14.5, leveling off at

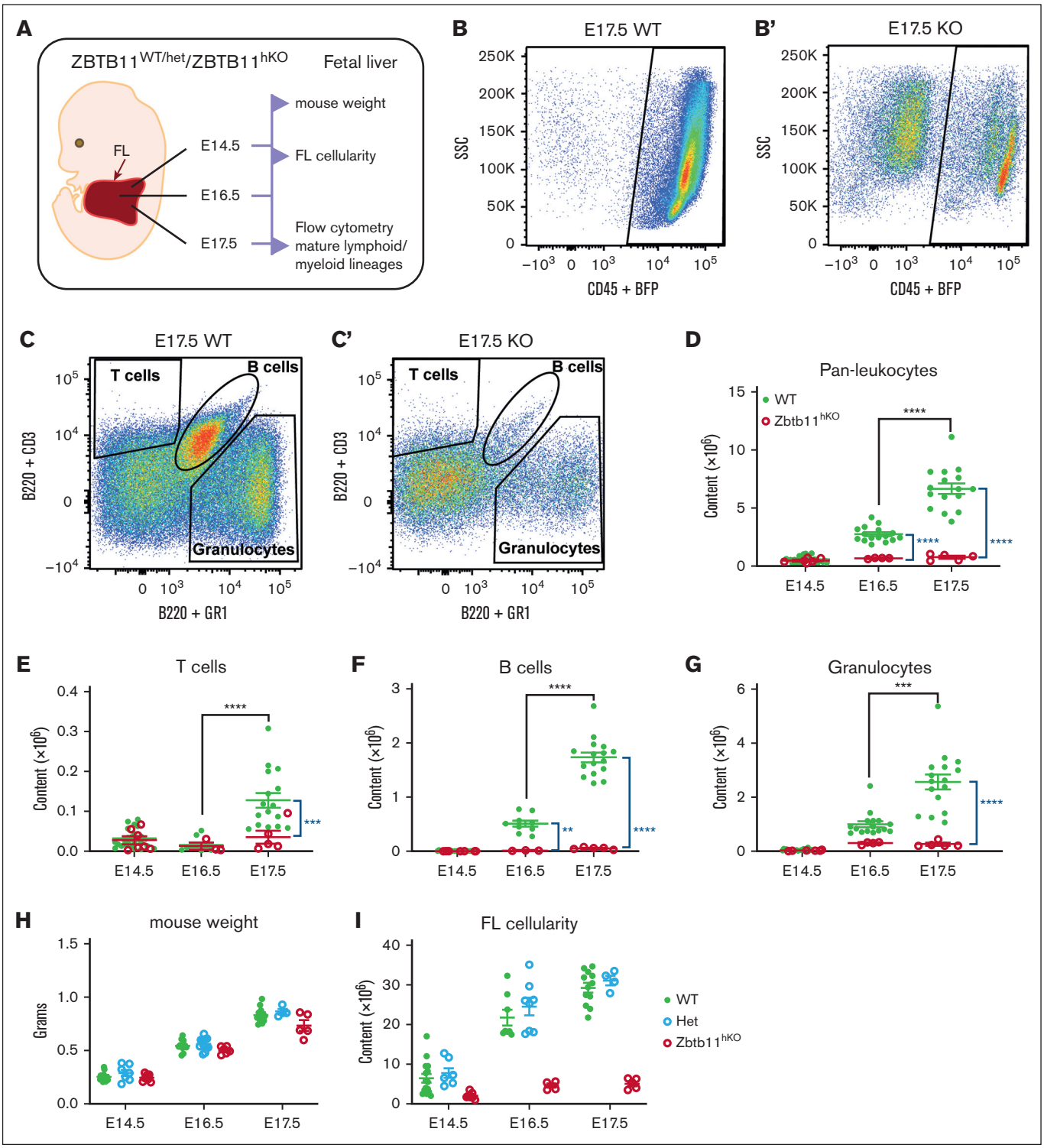

Figure 1. Homozygous Zbtb11 inactivation in the fetal hematopoietic compartment drastically impairs FL mature lymphoid and myeloid output. (A) Schematic description of the analysis. Flow cytometry analysis of FL at E17.5: dot plots showing the representative incidence of (B/B′) pan leukocytes (CD45$^+$); (C/C′) granulocytes (Gr1$^+$), T cells (CD3$^+$), and B cells (B220$^+$). Scatter plots showing the absolute quantification of total content at E14.5, E16.5, and E17.5: (D) CD45$^+$ leukocytes, (E) T cells, (F) B cells, and (G) granulocytes. Mouse embryo weight (H) and FL cellularity (I) showed no haploinsufficiency effect in heterozygotes. For panels D and G: E14.5 WT, n = 22 and KO, n = 7; E16.5 WT, n = 16 and KO, n = 4; E17.5 WT, n = 16 and KO, n = 5. For panels E and F: E14.5 WT, n = 22 and KO, n = 7; E16.5 WT, n = 9 and KO, n = 3; E17.5 WT, n = 16 and KO, n = 5. For panel H: E14.5 WT, n = 15, Het, n = 7, and KO n = 7; E16.5 WT, n = 10, Het, n = 12, and KO, n = 5; E17.5 WT, n = 12, Het, n = 4, and KO n = 4. For panel I: E14.5 WT, n = 15, Het, n = 7, and KO, n = 7; E16.5 WT, n = 8, Het, n = 8, and KO, n = 4; E17.5 WT, n = 12, Het, n = 4, and KO n = 5. WT/controls; (green); KO, *Zbtb11*^{hKO} (red); Het, *Zbtb11*$^{WT/hKO}$ (blue); data ± standard error of the mean. Two-way analysis of variance with Tukey (black) or Šídák (blue) multiple comparisons: $^{**}P < .01$; $^{***}P < .001$; $^{****}P < .0001$.

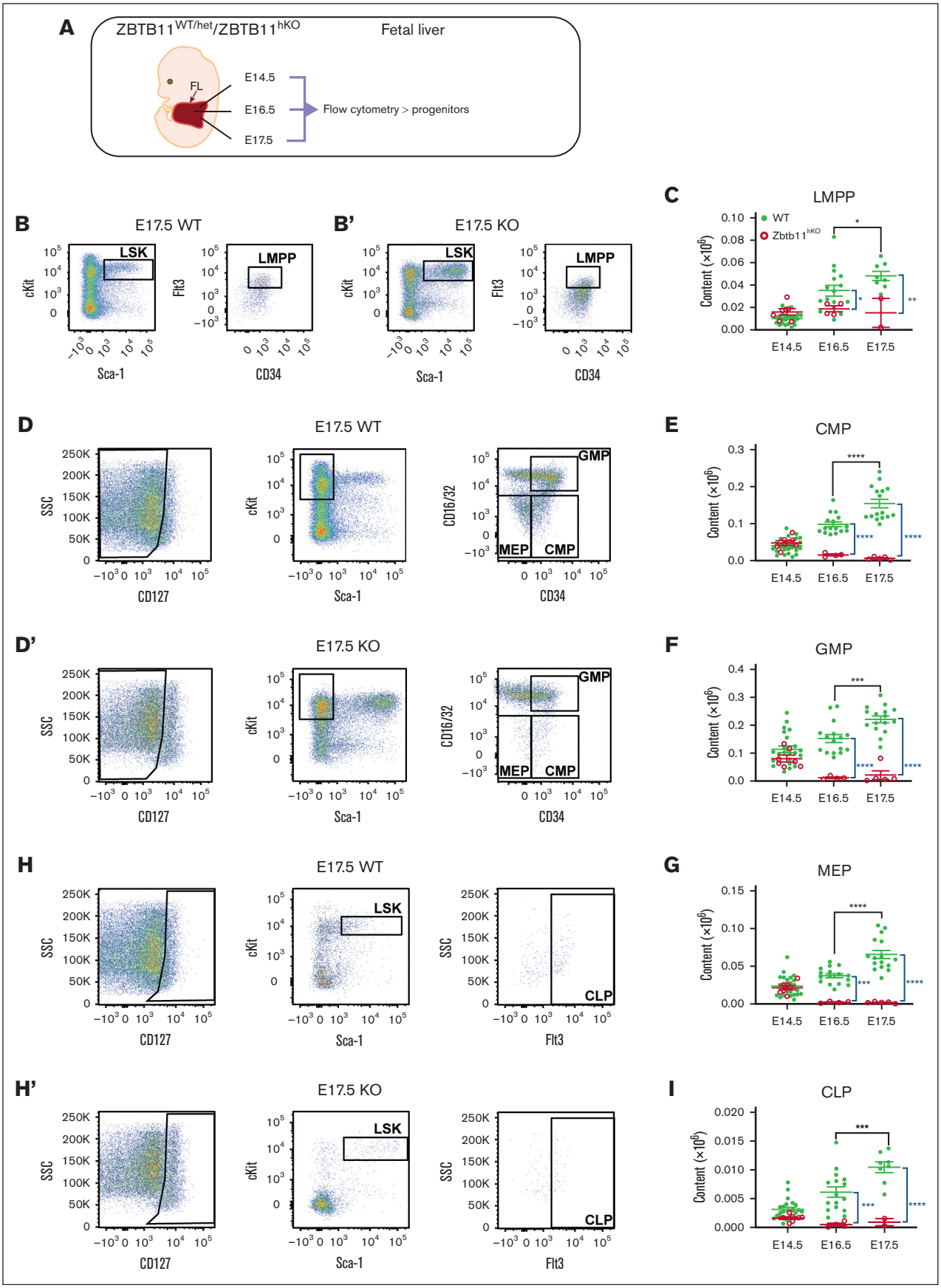
A
ZBTB11WT/het/ZBTB11hKO
Fetal liver
FL
E14.5
E16.5
E17.5
Flow cytometry > progenitors
B
E17.5 WT
LSK
LMPP
cKit
Flt3
Sca-1
CD34
B'
E17.5 KO
C
LMPP
WT
Zbtb11hKO
Content (×10^6)
E14.5
E16.5
E17.5
D
E17.5 WT
SSC
CD127
cKit
Sca-1
CD16/32
GMP
MEP
CMP
CD34
E
CMP
D'
E17.5 KO
F
GMP
H
E17.5 WT
CLP
G
MEP
H'
E17.5 KO
I
CLP

Figure 2.

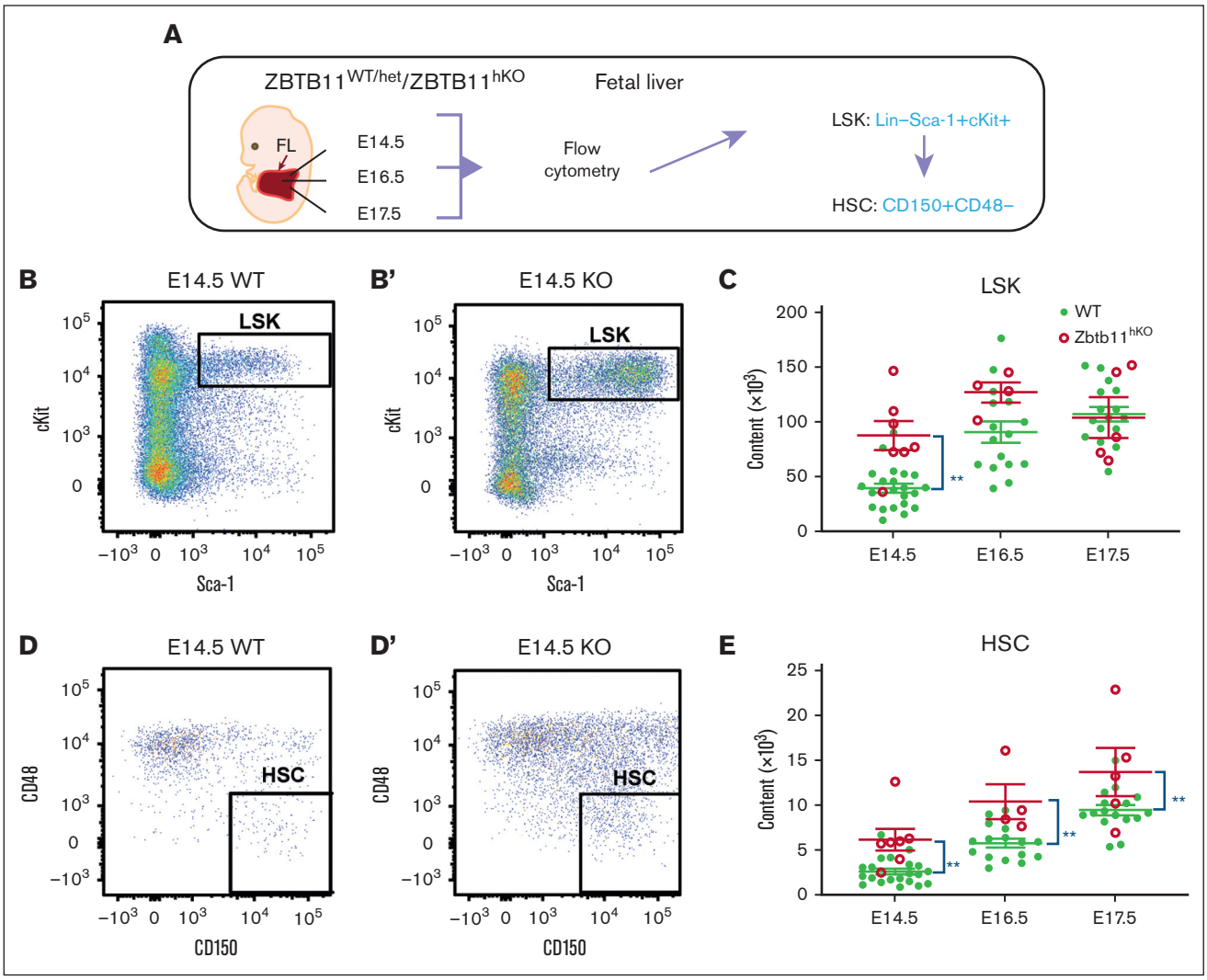

Figure 3. Multipotent *Zbtb11*^{hKO} progenitors and HSCs are elevated in the FL. (A) Schematic description of the analysis and definition of HSC used in all experiments. Flow cytometry analysis: (B/B′) HSC progenitors (LSK) and (D/D′) HSC (LSKCD150$^+$CD48$^-$) at E14.5, with dot plots showing the representative incidence. Scatter plots showing the absolute quantification at E14.5, E16.5, and E17.5: (C) total LSK (E14.5: *Zbtb11*^{hKO} = 8.7 × 10^4 (n = 7); controls = 3.9 × 10^4 [n = 22]; P = .0011), and (E) total HSC at E14.5 (*Zbtb11*^{hKO} = 6.1 × 10^3 [n = 7]; controls = 2.6 × 10^3 [n = 22]; P = .0072), E16.5 (*Zbtb11*^{hKO} = 10.4 × 10^3 [n = 4]; controls = 5.7 × 10^3 [n = 16]; P = .0062), and E17.5. (*Zbtb11*^{hKO} =13.7 × 10^3 [n = 5]; controls = 9.4 × 10^3 [n = 16]; P = .0061). WT/controls (green); KO, *Zbtb11*^{hKO} (red); data ± standard error of the mean. Two-way analysis of variance with Šídák multiple comparisons: **P < .01.

E16.5 and E17.5 (Figure 3B-C). Similarly, there were more *Zbtb11*^{hKO} phenotypic HSCs at E14.5, but HSC overabundance was sustained through E17.5 (Figure 3D-E). These observations provide strong evidence that the initial HSC specification in *Zbtb11*^{hKO} embryos is intact and that hematopoietic failure is not due to a lack of initial HSC specification but rather a failure of a downstream step incapacitating the development of a fully populated, multilineage hematopoietic system from the abundant number of HSCs that were initially specified. Given the near-100% excision efficiency of vav-iCre in embryonic development,[37] the very small but measurable number of lineage-committed progenitors that mostly decrease over time (Figure 2) may potentially arise from

Figure 2. In the absence of Zbtb11, FL-committed progenitor numbers fail to increase. (A) Schematic description of the analysis. Flow cytometry analysis dot plots show representative incidence at E17.5: (B/B′) LMPP (LSKCD34$^+$Flt3$^+$); (D/D′) CMP (Lin$^-$CD127$^-$Sca-1$^-$c-Kit$^+$CD34$^+$CD16/32$^-$), GMP (Lin$^-$CD127$^-$Sca-1$^-$c-Kit$^+$CD34$^+$CD16/32$^+$), and MEP (Lin$^-$CD127$^-$Sca-1$^-$c-Kit$^+$CD34$^-$CD16/32$^-$); and (H/H′) CLP (Lin$^-$CD127$^+$Sca-1$^+$cKit$^+$Flt3$^+$). Scatter plots showing the absolute quantification of total content at E14.5, E16.5, and E17.5: (C) LMPP, (E) CMP, (F) GMP, (G) MEP, and (I) CLP. For panels C and I: E14.5 WT, n = 22 and KO n = 7; E16.5 WT, n = 16 and KO n = 4; E17.5 WT, n = 8 and KO n = 2. For panels E-G: E14.5 WT, n = 22 and KO, n = 7; E16.5 WT, n = 16 and KO, n = 4; E17.5 WT, n = 16 and KO, n = 5. WT/controls (green); KO, *Zbtb11*^{hKO} (red); data ± standard error of the mean. Two-way analysis of variance with Tukey (black) or Šídák (blue) multiple comparisons: *P < .05; **P < .01; ***P < .001; ****P < .0001. CLP, common lymphoid progenitor; GMP, granulocyte–macrophage progenitor; LMPP, lymphoid-primed multipotent progenitor; MEP, myeloerythroid progenitor.

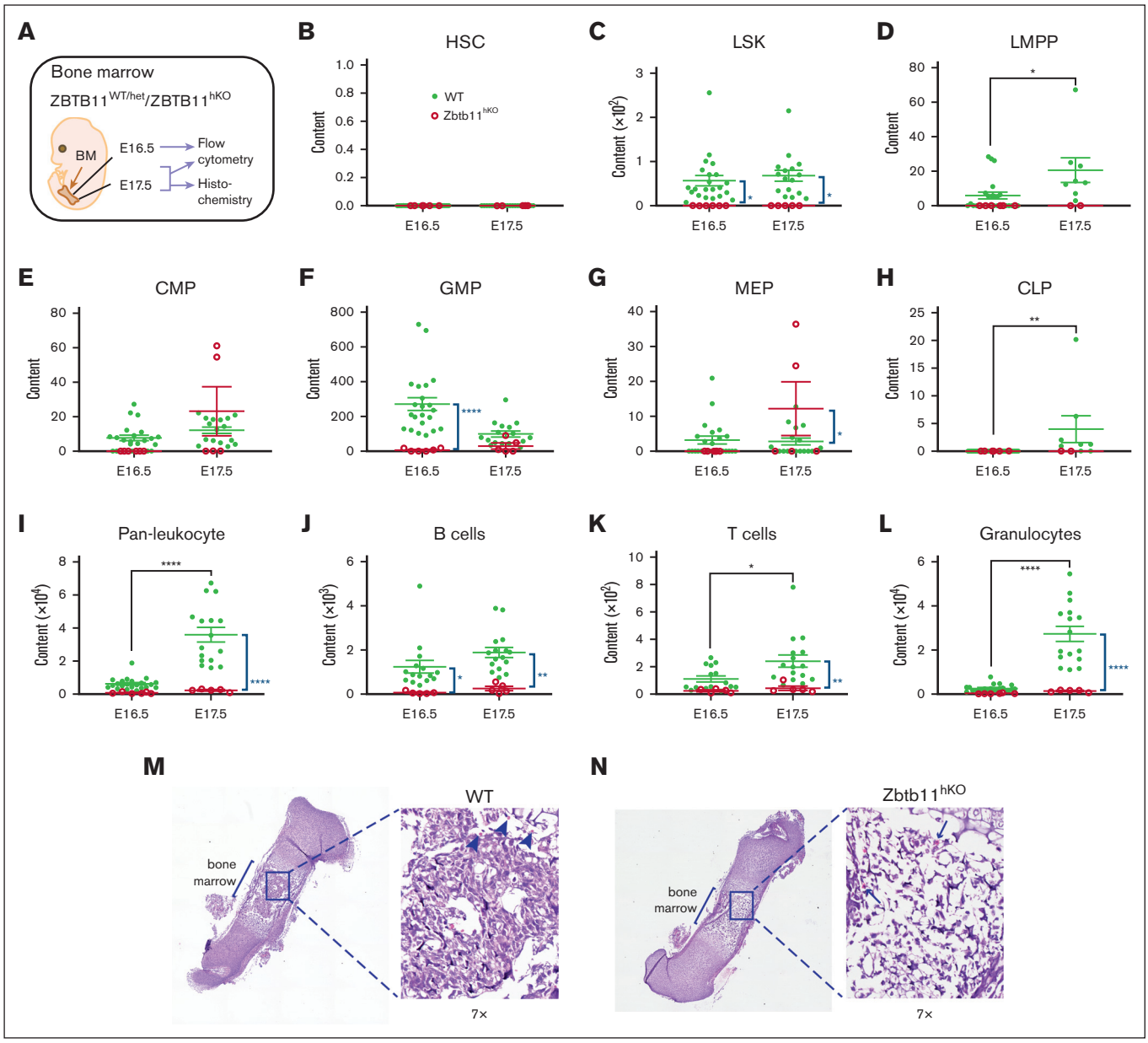

Figure 4. The absence of Zbtb11 in the hematopoietic compartment results in fetal BM failure. (A) Schematic description of the analysis. Scatter plots showing absolute quantification of total BM content at E16.5 and E17.5: (B) HSC, (C) LSK, (D) LMPP, (E) CMP, (F) GMP, (G) MEP (H), CLP, (I) pan leukocytes, (J) B cells, (K) T cells, and (L) granulocytes at E16.5 and E17.5. For panels B, C, E, F, G, I, and L: E16.5 WT, n = 22 and KO, n = 6; E17.5 WT, n = 16 description of the KO, n = 5. For panels D and H: E16.5 WT, n = 22 and KO, n = 6; E17.5 WT, n = 8 and KO, n = 2; For panels J and K: E16.5 WT, n = 15 and KO, n = 5; E17.5 WT, n = 16 and KO, n = 5. Hematoxylin and eosin staining of E17.5 femur sections for (M) WT and (N) *Zbtb11*^{hKO}. Insets are original magnification ×7 of boxed area. Arrowheads indicate enucleated erythroid cells (M), and arrows indicate nucleated erythroid cells (N). WT, wild-type controls (green); KO, *Zbtb11*^{hKO} (red); E, embryonic day; Data ± standard error of the mean. Two-way analysis of variance with Šídák multiple comparisons: *$P < .05$; **$P < .01$; ****$P < .0001$.

primitive HSC-independent progenitors. These may allow for limited lineage commitment but become depleted as development progressively relies on HSC-dependent hematopoiesis in a scenario where HSC function appears to be compromised.

Fetal BM failure occurs in the absence of Zbtb11

In mice, hematopoietic stem and progenitor cells migrate from the FL to seed the fetal BM, where hematopoiesis establishes gradually from at least E16.5.[38-40] Given the consistent elevation of *Zbtb11*^{hKO} HSC in FL, we investigated whether these HSCs could seed and initiate hematopoiesis in the fetal BM (Figure 4A). Although the establishment of fetal BM hematopoiesis occurred in control embryos as expected, there was near-complete failure of BM hematopoiesis in *Zbtb11*^{hKO} embryos (Figure 4B-L). In contrast to the FL, analysis of the fetal BM compartment showed that the *Zbtb11*^{hKO} LSK progenitor pool was absent through

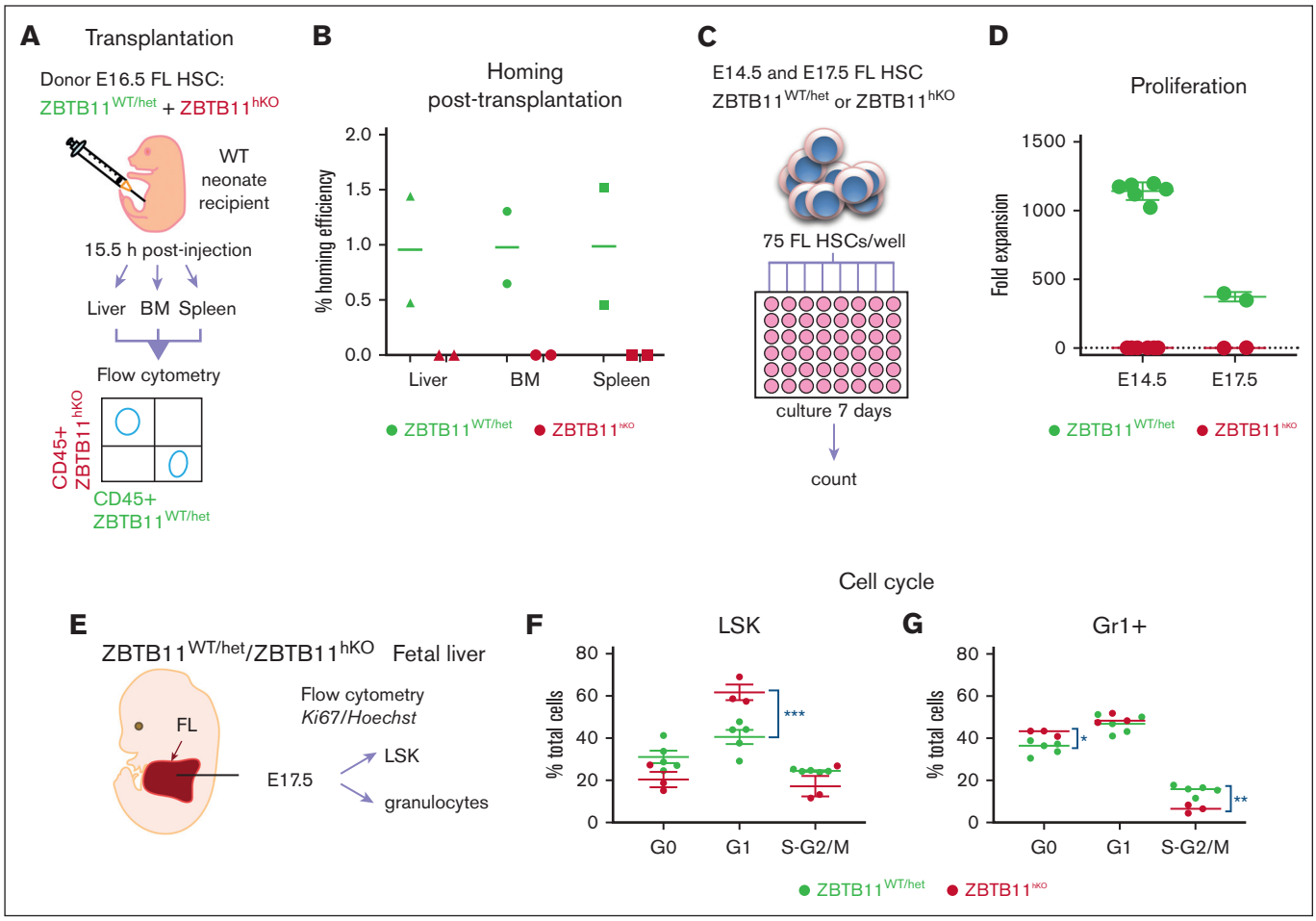

Figure 5. Functional failure of *Zbtb11*^{hKO} HSC: failure to home after transplantation, failure to proliferate in vitro, and impairment of cell cycle progression. (A) Schematic description of the transplantation and homing analysis. (B) Homing efficiency of E16.5 *Zbtb11*^{hKO} and WT FL HSCs transplanted into WT neonate. (C) Schematic description of the in vitro proliferation assay in which 75 immunophenotyped *Zbtb11*^{hKO} or WT FL HSCs were seeded per well and cultured in growth medium. Cells were counted in each well on day 7 and divided by 75 to determine the fold expansion. (D) Flow cytometry quantification of in vitro proliferation assays: on day 7, E14.5 HSC culture resulted in mean = 133 *Zbtb11*^{hKO} cells and 85 078 control cells, respectively; the average fold expansion was 1.78 and 1142.7 over initial seeding of 75 cells. (E) Schematic description of the cell cycle analysis. Cell cycle progression was assessed using the Ki67/nuclear DNA (Hoechst) ratio for (F) LSK and (G) granulocytes (Gr1^{+}) at E17.5. For panel B, n = 2 independent experiments. For panel D: E14.5 WT, n = 6 and KO, n = 6; E17.5 WT, n = 2 and KO, n = 2. For panels F and G: WT, n = 5 and KO, n = 3; WT/controls (green); KO, *Zbtb11*^{hKO} (red); data ± standard error of the mean. Two-way analysis of variance with Šidák multiple comparisons: *$P < .05$; **$P < .01$; ***$P < .001$.

E16.5-E17.5 (Figure 4C). Not surprisingly, this lack of *Zbtb11*^{hKO} LSK cells was accompanied by few, if any, BM-located committed progenitors (Figure 4D-H) and significantly fewer mature lineage cells (Figure 4I-L). Although the number of control hematopoietic cells underwent significant expansion from E16.5 to E17.5, *Zbtb11*^{hKO} hematopoietic cells did not (Figure 4D,H,I,K,L). Histology of fetal femurs showed disorganization and hypocellular marrow, concordant with the fluorescence-activated cell sorting (FACS) analysis (Figure 4M,N). Collectively, these data indicate that without Zbtb11, the FL to BM hematopoiesis transition does not occur, resulting in fetal BM failure.

Homing of *Zbtb11*^{hKO} HSCs is impaired

One reason for fetal BM failure could be defective homing of *Zbtb11*^{hKO} HSCs. To determine whether *Zbtb11*^{hKO} HSCs are capable of homing to hematopoietic tissues, a transplantation homing assay was performed. FAC-sorted, differentially labeled *Zbtb11*^{hKO} and control FL E16.5 HSCs were transplanted into a WT neonate by intraperitoneal injection. After 15.5 hours, hematopoietic organs were assayed for *Zbtb11*^{hKO} and control donor cells (Figure 5A). Although WT HSCs averaged ~1% homing efficiency, no *Zbtb11*^{hKO} donor cells were recoverable from the BM, spleen, or liver, indicating homing impairment of *Zbtb11*^{hKO} HSCs (Figure 5B). Hence, despite the overabundant *Zbtb11*^{hKO} HSCs in FL, these HSCs are unable to seed fetal BM even when transplanted to initiate hematopoiesis, contributing to hematopoietic failure in *Zbtb11*^{hKO} embryos.

Proliferation and cell cycle progression impairment in Zbtb11-deficient embryonic hematopoietic cells

Excessive proliferation of HSCs can result in their subsequent loss.[41,42] Given the increased number of *Zbtb11*^{hKO} HSC, we evaluated HSC proliferation directly by a 7-day in vitro culture assay seeded with 75 E14.5 or E17.5 FAC-sorted HSCs (Figure 5C).

At this stage, HSC are still highly proliferative.[3,43] The hematopoietic cell output of HSCs, as measured based on the number of cells per well, was increased >1000-fold in the WT cultures but not in the *Zbtb11*^{hKO} cultures, which were less than doubled at E14.5 (Figure 5D; average = 133 per well). Cell death could not account for the failure of *Zbtb11*^{hKO} cell numbers to expand because there were slightly more cells at the end of the assay than at the beginning (75 per well). However, at E17.5, 5 out of 6 wells seeded with *Zbtb11*^{hKO} HSCs had no viable cells on day 7, suggesting that cell survival was compromised and that cell death largely contributed to the proliferation failure of these older HSCs.

Cell cycle progression in HSCs is very tightly regulated, and adult HSCs can remain quiescent for long periods.[44] Because Zbtb11 loss completely arrests cell cycle progression in zebrafish,[18] we examined these processes in murine *Zbtb11*^{hKO} hematopoietic cells (Figure 5E). At E17.5, a greater proportion of *Zbtb11*^{hKO} FL LSK multipotent progenitors accumulated in G_1 than in controls (Figure 5F). Of the cells capable of differentiating along the granulocyte lineage, a significantly higher proportion of *Zbtb11*^{hKO} cells were quiescent (G_0), accompanied by a reduced proportion progressing to the S/M phase (Figure 5G). This is consistent with our previous zebrafish 5-ethynyl 2′-deoxyuridine incorporation data showing cell cycle arrest before the S phase[18] and demonstrates that Zbtb11 is specifically required for cell cycle progression in the mouse hematopoietic compartment. Because cell death did not increase in E14.5 *Zbtb11*^{hKO} HSCs, the lack of in vitro proliferation was likely due to checkpoint restriction. At E17.5, checkpoint restriction may initially impair proliferation (G_1 accumulation; Figure 5F) but becomes more severe, causing cells to exit the cell cycle (G_0 accumulation and decreased division; Figure 5G) and ultimately undergo cell death, as observed in HSCs in the in vitro proliferation assay at E17.5. This suggests that the overabundance of *Zbtb11*^{hKO} FL HSCs may arise from increased specification rather than aberrant self-renewal.

In the absence of Zbtb11, phenotypic HSC lack an erythroid-primed subpopulation, and niche and OXPHOS gene signatures are downregulated

Unsupervised clustering of E14.5 *Zbtb11*^{hKO} and control FL HSC single-cell RNAseq (scRNAseq) generated k = 5 clusters: 2 in which *Zbtb11*^{hKO} HSCs were underrepresented (1 and 3), 2 in which *Zbtb11*^{hKO} HSCs were overrepresented (0 and 4) and 1 cluster (2) in which *Zbtb11*^{hKO} and control HSCs were balanced (Figure 6A-B). Cells were classified into the cell cycle phase based on gene expression data ratios,[45] and most cells were in G_1 (WT = 71.1%, KO = 68.1%). Although there was no significant difference in the proportion of cells assigned to each cell cycle phase based on the genotype ($G_{2/M}$: WT = 18.9% and KO = 19.8%; S: WT = 10.0% and KO = 12.1%), the proportion of cells within each cluster was separable based on the cell cycle (Figure 6D). Differential gene expression between clusters revealed upregulation of erythroid genes in cluster 1, suggesting a subpopulation of erythroid-primed HSCs (Figure 6C). When the expression of marker genes for each cluster was evaluated across individual hematopoietic lineages defined in the hemosphere,[46] marked enrichment for erythroid lineage signature genes occurred only in cluster 1 (Figure 6E; supplemental Figure 4A-D). Furthermore, GO analysis showed enrichment for erythropoiesis in cluster 1 (supplemental Figure 4E), revealing a subpopulation in this cluster poised for differentiation along the erythroid lineage.[47] Because cluster 1 mainly comprised control HSCs (Figure 6A), this uncovered a potential genetic signature underlying the profound early anemia of *Zbtb11*^{hKO} embryos. Indeed, the E17.5 *Zbtb11*^{hKO} BM showed only nucleated erythroid cells, indicating a delay or arrest in erythrocyte development in the absence of Zbtb11 (Figure 4N). Because *Zbtb11*^{hKO} HSCs were abundantly specified but hematopoiesis failed, we examined whether there was a disruption in genes associated with the HSC niche. Figure 6F shows the downregulation of several families of genes crucial for the correct trafficking of HSCs to the FL, including receptor tyrosine kinases (Flt3), adhesion molecules (integrins and cadherin 5), cytokine receptors (colony stimulating factor receptors), and transcription factors (Runx1 [RUNX family transcription factor 1, also known as Acute Myeloid Leukemia 1 (AML1)] and RUNX1 partner transcriptional corepressor 1 [Runx1T].; interferon regulatory factors). Furthermore, c-Kit and Flt3 cell surface proteins were correspondingly decreased in LSK populations (Figure 6G,H).

Clusters were analyzed for GO terms and KEGG pathway enrichment (supplemental Figure 5A-E). The cells in cluster 0 were predominantly *Zbtb11*^{hKO} HSCs. Interestingly, one of the most overrepresented pathways in this cluster was necroptosis (supplemental Figure 5A), a caspase-independent genetically programmed form of cell death.[48] Cluster 3 cells were all in G_1 phase, and GO analysis showed enrichment of terms associated with nucleoside triphosphate metabolism, adenosine triphosphate synthesis and metabolism, and respiratory transport chain, supported by KEGG pathway analysis, in which OXPHOS was in the top 10 terms (supplemental Figure 5D). This likely reflects cells in G_1 undergoing preparation for DNA synthesis. Both clusters (1 and 3), which were predominantly composed of control HSCs, showed enrichment of gene signatures for OXPHOS and metabolic pathways (supplemental Figure 5B,D). These gene signatures were not enriched in clusters predominantly lacking functional Zbtb11, suggesting that these pathways may be defective in *Zbtb11*^{hKO} HSCs. Interestingly, cluster 4, consisting predominantly of *Zbtb11*^{hKO} HSCs, showed enrichment of GO terms for DNA repair, replication, cellular response to DNA damage stimulus, and cellular response to stress (supplemental Figure 5E). This was supported by the disproportionate enrichment of 5 KEGG pathways involved in DNA repair: base excision, nucleotide excision, mismatch repair, homologous recombination, and the Fanconi anemia pathway as well as DNA replication and pyrimidine metabolism. These analyses revealed susceptibility to DNA damage and potential replicative stress in this subpopulation of *Zbtb11*^{hKO} HSCs.

Discussion

We have shown that Zbtb11 is a key regulator of the HSC function required for self-renewal and differentiation. Zbtb11 ablation during murine hematopoietic development generated overabundant HSCs in FL, yet profound BM failure and embryonic lethality followed. The intricacies of this severe disturbance in HSC function warrant further investigation because the requirement for Zbtb11 and its regulatory networks present an attractive avenue for therapeutic manipulation in HSC-directed therapies. Currently, it is unknown whether the overabundance of HSCs in Zbtb11-depleted hematopoietic compartments results from increased specification or increased cycling before E14.5, leading to HSC exhaustion by E14.5. Failure of transplanted *Zbtb11*^{hKO} HSCs to home to major

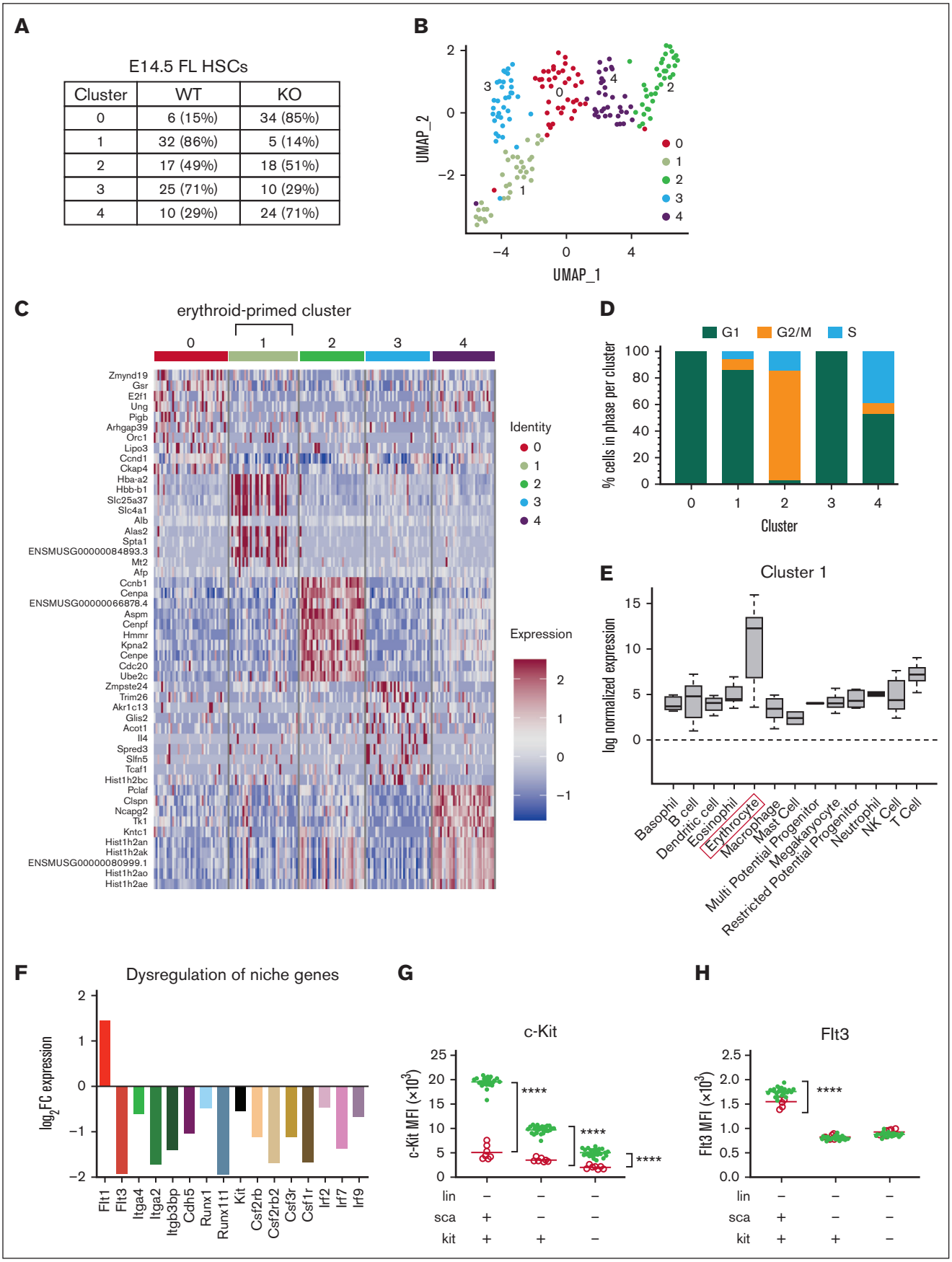
A
E14.5 FL HSCs
Cluster | WT | KO
0 | 6 (15%) | 34 (85%)
1 | 32 (86%) | 5 (14%)
2 | 17 (49%) | 18 (51%)
3 | 25 (71%) | 10 (29%)
4 | 10 (29%) | 24 (71%)
B
UMAP_2
UMAP_1
C
erythroid-primed cluster
Identity
Expression
D
G1
G2/M
S
% cells in phase per cluster
Cluster
E
Cluster 1
log normalized expression
Basophil
B cell
Dendritic cell
Eosinophil
Erythrocyte
Macrophage
Mast Cell
Multi Potential Progenitor
Megakaryocyte
Restricted Potential Progenitor
Neutrophil
NK Cell
T Cell
F
Dysregulation of niche genes
log2FC expression
Flt1
Flt3
Itga4
Itga2
Itgb3bp
Cdh5
Runx1
Runx1t1
Kit
Csf2rb
Csf2rb2
Csf3r
Csf1r
Irf2
Irf7
Irf9
G
c-Kit
c-Kit MFI (×10³)
lin
sca
kit
H
Flt3
Flt3 MFI (×10³)

Figure 6.

hematopoietic organs could arise from HSC death or insensitivity to homing signaling pathways. In vitro studies suggest that E14.5 *Zbtb11*^{hKO} HSCs are quiescent and that *Zbtb11*^{hKO} HSCs mostly do not survive by E17.5; however, it is possible that E16.5 *Zbtb11*^{hKO} HSCs survive in vivo for a short duration in the homing study. Another important question is whether Zbtb11 affects the capacity of HSCs to exit FL, given the accumulation of *Zbtb11*^{hKO} HSCs in FL but a shift to significantly fewer *Zbtb11*^{hKO} lineage-committed progenitors over time. The inability of transplanted E16.5 *Zbtb11*^{hKO} HSCs to home to hematopoietic organs in a WT recipient precludes additional classical transplantation studies to dissect HSC function in this model. In future studies, inducible models of Zbtb11 deletion in HSCs and specific mature hematopoietic lineages will determine the precise onset of Zbtb11 requirement, function of Zbtb11 in adult HSCs, and whether the impact observed in mature lineages in *Zbtb11*^{hKO} is due to defective HSCs and/or a cell-intrinsic Zbtb11 requirement in some or all of these lineages.

Increased specification of HSCs followed by complete BM failure is an uncommon phenotype. Ablation of geminin is one example in which HSCs increase but at a cost of proliferation and differentiation of lineage-committed progenitors, postulated to occur through the epigenetic regulation of multipotency vs lineage specification genetic programs.[49] We previously showed that Zbtb11 is under the regulatory control of myeloid transcription factors Pu.1, Gfi1a, Gfi1b, and C/ebpα.[18] Hematopoiesis-specific transcriptional binding partners remain to be identified for Zbtb11, and determining these would provide further mechanistic insight along with interrogating Zbtb11-mediated alterations in the hematopoietic gene regulatory landscape.

The crucial role played by mitochondrial reactive oxygen species (ROS) in regulating HSC fate and its therapeutic application is currently a topic of much interest.[50,51] Changes in OXPHOS and its byproduct, ROS, determine the balance between HSC self-renewal and differentiation, with a switch to OXPHOS needed to support the metabolic demands of differentiating HSCs.[52-56] Both scRNAseq of mouse HSCs and our bulk RNAseq of Zbtb11-deficient zebrafish neutrophils showed significantly affected OXPHOS and mitochondrial pathways (supplemental Figure 5A-B,D-F),[18] concordant with reports in *Zbtb11*$^{-/-}$ mouse embryonic stem cells.[27,57] A recent study showed that Zbtb11 is required for mouse embryonic stem cell pluripotency by maintaining the repression of poised prodifferentiation genes.[27] However, *Zbtb11*^{hKO} HSCs, which are overabundant yet intrinsically incompetent to undergo differentiation and proliferation, appear to have lost multipotency or the function of key cellular components, such as respiratory complex I and mitoribosome,[57] required for the execution of differentiation programs. Cluster 4 showed an increase in genes responsible for DNA damage repair, suggesting these HSCs are likely under replicative stress, consistent with their accumulation in the S phase (Figure 6D; supplemental Figure 5E). This ties in with the dysregulation of OXPHOS/ROS and suboptimal metabolic requirements for replication, which may exacerbate the failure of *Zbtb11*^{hKO} HSCs to progress through the intra-S-phase checkpoint.[58] Notably, *Zbtb11*^{hKO} and mitochondrial phosphatase *Ptpmt1*$^{-/-}$ HSCs share a similar phenotype.[55] Measuring ROS, adenosine triphosphate, and oxygen consumption in *Zbtb11*^{hKO} HSCs and the remaining lineage-committed and mature cells could elucidate Zbtb11-mediated defects in mitochondrial function as a source of failed hematopoiesis. Together, these observations highlight the potential role of Zbtb11 in regulating mitochondrial activity in HSC.

During murine development, the first wave of primitive hematopoiesis occurs in the yolk sac between E7.5 and E9.5 to sustain the early embryonic tissues. Around E9, a definitive (late fetal/adult) population of erythroid-myeloid progenitors capable of forming a broader range of lineages also emerges in the yolk sac.[59] Zbtb11 expression has been detected in the brain or central nervous system and several other organs during the relevant stages of HSC specification.[60] Importantly, Zbtb11 is expressed in the yolk sac (8.9), aorta-gonads-mesonephros (7.4), placenta (8.8), and FL (E12.5 = 8.5; E13.5 = 8.2; E14.5 = 7.4; mean expression of replicate samples, StemSite[61]). Our studies demonstrate that when Zbtb11 is deleted in the hematopoietic compartment, there is a loss of an erythroid subpopulation, evidenced by predominantly WT erythroid signature-expressing HSCs in cluster 1, early FL anemia, and the presence of only immature nucleated erythroid cells at E17.5 in the BM. Therefore, it is interesting to speculate whether ZBTB11 acts in the FL microenvironment to support the differentiation of yolk sac-derived erythroid-myeloid progenitors, which are thought to be the source for the establishment of the adult hematopoietic system in this niche. Vav-Cre expression initiates at approximately E11.5;[62] therefore, earlier hematopoietic development in the yolk sac, including specification of erythroid-myeloid progenitors, will not be affected by Zbtb11 loss in this vav-iCre deletion-dependent model. However, at E14.5, while HSCs were within the FL niche, Zbtb11 loss in HSCs resulted in dysregulation of key genes involved in hematopoietic differentiation and proliferation and cell-cell interactions, including c-Kit and Flt3. In HSCs, c-Kit acts to preserve self-renewal,[63,64] with c-Kit density inversely correlated with stemness.[64,65] A fourfold decrease in the mean fluorescence intensity of c-Kit cell surface protein expression in *Zbtb11*^{hKO} LSK cells at E14.5 suggested that c-Kit signaling

Figure 6. scRNAseq analysis of WT and *Zbtb11*^{hKO} HSCs reveals underrepresentation of *Zbtb11*^{hKO} HSCs in the cluster characterized by an erythroid signature and dysregulation of niche gene expression. (A) Distribution of cells based on the number, proportion (%), and genotype for each cluster. Clusters 1 and 3 are disproportionately comprised of WT cells, whereas clusters 0 and 4 are disproportionately comprised of KO cells. (B) Uniform Manifold Approximation and Projection plot of unsupervised clustering identified 5 subpopulations of E14.5 FL HSCs (LSK/SLAM). (C) Heatmap of normalized log-expression values for the top 10 cluster-specific marker genes. Column colors represent the cluster identity to which each cell is assigned. (D) Distribution of cell cycle phase within each cluster. (E) Enrichment of log normalized gene expression of top 10 upregulated genes in each cluster was evaluated across individual hematopoietic lineages defined using the Haemopedia Mouse RNAseq data set, which contains 129 samples classified into 13 cell lineages and 57 cell types.[46] Expression of marker genes for cluster 1 shows enrichment for erythrocyte lineage (boxed) genes. (F) Differential expression of hematopoietic niche genes in unclustered E14.5 FL *Zbtb11*^{hKO} HSCs compared with WT HSCs. Y-axis shows the $\log_2$FC (fold change) gene expression level, with a false discovery rate < 0.05. Mean fluorescence intensity (MFI) of c-Kit (G) and Flt3 (H) protein in *Zbtb11*^{hKO} and WT control progenitors at E14.5. WT/controls (green); KO, (red); fluorescence intensity of the protein is shown along the y-axis; data ± standard error of the mean. Two-way analysis of variance with Šídák multiple comparisons: ****$P < .0001$.

disruption could contribute to the inhibition of *Zbtb11*^{hKO} stem and progenitor differentiation (Figure 6G). Consistent with this, unclustered scRNAseq showed that c-Kit was underexpressed in *Zbtb11*^{hKO} HSCs (Figure 6F), whereas kit ligand expression was normal. Flt3 is also crucial for hematopoietic development and mutations in this gene are commonly associated with acute myeloid leukemia.[66-68] The downregulation of both c-Kit and Flt3 in *Zbtb11*^{hKO} progenitor cells and multiple other factors that support HSC differentiation and expansion (Figure 6F-H) highlight the role of Zbtb11 in maintaining a gene regulatory landscape permitting HSCs to functionally interact with their microenvironment.

In conclusion, these data demonstrate an absolute requirement for Zbtb11 to sustain murine fetal hematopoiesis after HSCs are specified. This requirement for Zbtb11 acts through cell-essential mechanisms affecting HSC homing, proliferation, and mitochondrial function and the regulatory gene networks required for productive hematopoietic output from the hematopoietic niche.

Acknowledgments

The authors thank the FlowCore and Monash Animal Research Platform for their equipment and technical support. The authors thank Jeanette Rientjes from Gene Recombineering (Monash) and Arianna Nenci from the Monash Gene Technology Facility, Jessica Hatwell-Humble for mouse husbandry and technical expertise, Brenda Williams and Madeline Fulton for technical expertise, Chad Heazlewood for histology, and Tracey Baldwin from Single Cell Open Research Endeavour (The Walter and Eliza Hall Institute of Medical Research) for technical assistance.

This work was supported by the National Health and Medical Research Council (1070687) (G.J.L. and M.C.K.), Cancer Council Victoria (1047660) (G.J.L. and M.C.K.), National Institutes of Health (R01 HL079545) (G.J.L.), and the La Trobe Institute for Molecular Science, VIC Australia (M.C.K.). The Australian Regenerative Medicine Institute is supported by funds from the State Government of Victoria and the Australian Federal Government.

Authorship

Contribution: M.C.K., S.K.N., and G.J.L. conceptualized the study; H.C., B.C., S.K.N., and M.C.K. conducted the experiments; M.C.K., H.C., B.C., S.K.N., P.H., S.H.N., and A.S. performed the formal analysis; D.A.-Z. and S.H.N. provided resources for the scRNAseq; M.C.K., S.K.N., and G.J.L. supervised the study; M.C.K. and G.J.L. wrote the original draft of the manuscript; M.C.K., S.K.N., and G.J.L. acquired funding; and all authors contributed to the review and editing process.

Conflict-of-interest disclosure: The authors declare no competing financial interests.

ORCID profiles: S.H.N., 0000-0003-0299-3301; D.A.-Z., 0000-0003-4928-1846; P.H., 0000-0002-8153-6258; A.S., 0000-0003-3999-7701; B.C., 0000-0002-3024-3893; M.C.K., 0000-0001-8141-4069; G.J.L., 0000-0003-0325-798X.

Correspondence: Graham J. Lieschke, Australian Regenerative Medicine Institute, Level 1, Building 75 Monash University, Wellington Road, Clayton, VIC 3800, Australia; email: graham.lieschke@monash.edu; and M. Cristina Keightley, La Trobe Rural Health School, La Trobe University, PO Box 199, Bendigo, VIC 3552, Australia; email: c.keightley@latrobe.edu.au.

References

1. Till JE, McCulloch EA. A direct measurement of the radiation sensitivity of normal mouse bone marrow cells. *Radiat Res*. 2012;178(2):213-222.
2. Siminovitch L, McCulloch EA, Till JE. The distribution of colony-forming cells among spleen colonies. *J Cell Comp Physiol*. 1963;62(3):327-336.
3. Morrison SJ, Hemmati HD, Wandycz AM, Weissman IL. The purification and characterization of fetal liver hematopoietic stem cells. *Proc Natl Acad Sci U S A*. 1995;92(22):10302-10306.
4. Weissman IL. Stem cells: units of development, units of regeneration, and units in evolution. *Cell*. 2000;100(1):157-168.
5. Cheng T, Rodrigues N, Shen H, et al. Hematopoietic stem cell quiescence maintained by p21cip1/waf1. *Science*. 2000;287(5459):1804-1808.
6. Marks-Bluth J, Pimanda JE. Cell signalling pathways that mediate haematopoietic stem cell specification. *Int J Biochem Cell Biol*. 2012;44(12):2175-2184.
7. Orkin SH, Zon LI. Hematopoiesis: an evolving paradigm for stem cell biology. *Cell*. 2008;132(4):631-644.
8. Tang C, Westling J, Seto E. trans repression of the human metallothionein IIA gene promoter by PZ120, a novel 120-kilodalton zinc finger protein. *Mol Cell Biol*. 1999;19(1):680-689.
9. Siggs OM, Beutler B. The BTB-ZF transcription factors. *Cell Cycle*. 2012;11(18):3358-3369.
10. Kelly K, Daniel J. POZ for effect – POZ-ZF transcription factors in cancer and development. *Trends Cell Biol*. 2006;16(11):578-587.
11. Maeda T. Regulation of hematopoietic development by ZBTB transcription factors. *Int J Hematol*. 2016;104(3):310-323.
12. Chevrier S, Corcoran LM. BTB-ZF transcription factors, a growing family of regulators of early and late B-cell development. *Immunol Cell Biol*. 2014;92(6):481-488.
13. Punwani D, Simon K, Choi Y, et al. Transcription factor zinc finger and BTB domain 1 is essential for lymphocyte development. *J Immunol*. 2012;189(3):1253-1264.
14. Sakurai N, Maeda M, Lee SU, et al. The LRF transcription factor regulates mature B cell development and the germinal center response in mice. *J Clin Invest*. 2011;121(7):2583-2598.
15. Bilic I, Ellmeier W. The role of BTB domain-containing zinc finger proteins in T cell development and function. *Immunol Lett*. 2007;108(1):1-9.

16. He X, He X, Dave VP, et al. The zinc finger transcription factor Th-POK regulates CD4 versus CD8 T-cell lineage commitment. *Nature*. 2005;433(7028):826-833.
17. Shaffer AL, Yu X, He Y, Boldrick J, Chan EP, Staudt LM. BCL-6 represses genes that function in lymphocyte differentiation, inflammation, and cell cycle control. *Immunity*. 2000;13(2):199-212.
18. Keightley MC, Carradice DP, Layton JE, et al. The Pu.1 target gene Zbtb11 regulates neutrophil development through its integrase-like HHCC zinc finger. *Nat Commun*. 2017;8:14911.
19. Nie W, Hu MJ, Zhang Q, et al. DUBR suppresses migration and invasion of human lung adenocarcinoma cells via ZBTB11-mediated inhibition of oxidative phosphorylation. *Acta Pharmacol Sin*. 2022;43(1):157-166.
20. Yu K, Li Q, Cheng Q, et al. MicroRNA-548j inhibits type I interferon production by targeting ZBTB11 in patients with chronic hepatitis B. *Biochem Biophys Res Commun*. 2017;488(4):628-633.
21. Yan X, Chen Z, Brechot C. The differences in gene expression profile induced by genotype 1b hepatitis C virus core isolated from liver tumor and adjacent non-tumoral tissue. *Hepat Mon*. 2011;11(4):255-262.
22. Zhang X, Chu H, Wen L, et al. Competing endogenous RNA network profiling reveals novel host dependency factors required for MERS-CoV propagation. *Emerg Microbes Infect*. 2020;9(1):733-746.
23. Sumathipala D, Stromme P, Fattahi Z, et al. ZBTB11 dysfunction: spectrum of brain abnormalities, biochemical signature and cellular consequences. *Brain*. 2022;145(7):2602-2616.
24. Scala M, De Grandis E, Nobile G, et al. Biallelic ZBTB11 variants associated with complex neuropsychiatric phenotype featuring Tourette syndrome. *Brain*. 2023;146(1):e1-e4.
25. Harripaul R, Vasli N, Mikhailov A, et al. Mapping autosomal recessive intellectual disability: combined microarray and exome sequencing identifies 26 novel candidate genes in 192 consanguineous families. *Mol Psychiatry*. 2018;23(4):973-984.
26. Fattahi Z, Sheikh TI, Musante L, et al. Biallelic missense variants in ZBTB11 can cause intellectual disability in humans. *Hum Mol Genet*. 2018;27(18):3177-3188.
27. Garipler G, Lu C, Morrissey A, et al. The BTB transcription factors ZBTB11 and ZFP131 maintain pluripotency by repressing pro-differentiation genes. *Cell Rep*. 2022;38(11):110524.
28. Chen L, Liu Z, Tang H, et al. Knockdown of ZBTB11 impedes R-loop elimination and increases the sensitivity to cisplatin by inhibiting DDX1 transcription in bladder cancer. *Cell Prolif*. 2022;55(12):e13325.
29. Boogerd CJ, Lacraz GPA, Vertesy A, et al. Spatial transcriptomics unveils ZBTB11 as a regulator of cardiomyocyte degeneration in arrhythmogenic cardiomyopathy. *Cardiovasc Res*. 2023;119(2):477-491.
30. Abram CL, Roberge GL, Hu Y, Lowell CA. Comparative analysis of the efficiency and specificity of myeloid-Cre deleting strains using ROSA-EYFP reporter mice. *J Immunol Methods*. 2014;408:89-100.
31. Siegemund S, Shepherd J, Xiao C, Sauer K. hCD2-iCre and vav-iCre mediated gene recombination patterns in murine hematopoietic cells. *PLoS One*. 2015;10(4):e0124661.
32. Behringer R, Gertsenstein M, Nagy KV, Nagy A. *Production of Transgenic Mice by Pronuclear Microinjection*. *Manipulating The Mouse Embryo: A Laboratory Manual*. 4th ed. New York: Cold Spring Harbor Laboratory Press; 2014.
33. Cao H, Williams B, Nilsson SK. Investigating the interaction between hematopoietic stem cells and their niche during embryonic development: optimizing the isolation of fetal and newborn stem cells from liver, spleen, and bone marrow. *Methods Mol Biol*. 2014;1185:9-20.
34. Grassinger J, Haylock DN, Williams B, Olsen GH, Nilsson SK. Phenotypically identical hemopoietic stem cells isolated from different regions of bone marrow have different biologic potential. *Blood*. 2010;116(17):3185-3196.
35. Hashimshony T, Senderovich N, Avital G, et al. CEL-Seq2: sensitive highly-multiplexed single-cell RNA-Seq. *Genome Biol*. 2016;17:77.
36. Lau KX, Mason EA, Kie J, et al. Unique properties of a subset of human pluripotent stem cells with high capacity for self-renewal. *Nat Commun*. 2020;11(1):2420.
37. Neo WH, Booth CAG, Azzoni E, et al. Cell-extrinsic hematopoietic impact of Ezh2 inactivation in fetal liver endothelial cells. *Blood*. 2018;131(20):2223-2234.
38. Christensen JL, Wright DE, Wagers AJ, Weissman IL. Circulation and chemotaxis of fetal hematopoietic stem cells. *PLoS Biol*. 2004;2(3):E75.
39. Coşkun S, Chao H, Vasavada H, et al. Development of the fetal bone marrow niche and regulation of HSC quiescence and homing ability by emerging osteolineage cells. *Cell Rep*. 2014;9(2):581-590.
40. Gekas C, Dieterlen-Lievre F, Orkin SH, Mikkola HK. The placenta is a niche for hematopoietic stem cells. *Dev Cell*. 2005;8(3):365-375.
41. Wilson A, Oser GM, Jaworski M, et al. Dormant and self-renewing hematopoietic stem cells and their niches. *Ann N Y Acad Sci*. 2007;1106:64-75.
42. Yanai H, Beerman I. Proliferation: driver of HSC aging phenotypes? *Mech Ageing Dev*. 2020;191:111331.
43. Ikuta K, Weissman IL. Evidence that hematopoietic stem cells express mouse c-kit but do not depend on steel factor for their generation. *Proc Natl Acad Sci U S A*. 1992;89(4):1502-1506.
44. Cheshier SH, Morrison SJ, Liao X, Weissman IL. In vivo proliferation and cell cycle kinetics of long-term self-renewing hematopoietic stem cells. *Proc Natl Acad Sci U S A*. 1999;96(6):3120-3125.

45. Scialdone A, Natarajan KN, Saraiva LR, et al. Computational assignment of cell-cycle stage from single-cell transcriptome data. *Methods*. 2015;85:54-61.
46. de Graaf CA, Choi J, Baldwin TM, et al. Haemopedia: an expression atlas of murine hematopoietic cells. *Stem Cell Rep*. 2016;7(3):571-582.
47. Nestorowa S, Hamey FK, Pijuan Sala B, et al. A single-cell resolution map of mouse hematopoietic stem and progenitor cell differentiation. *Blood*. 2016;128(8):e20-31.
48. Linkermann A, Green DR. Necroptosis. *N Engl J Med*. 2014;370(5):455-465.
49. Karamitros D, Patmanidi AL, Kotantaki P, et al. Geminin deletion increases the number of fetal hematopoietic stem cells by affecting the expression of key transcription factors. *Development*. 2015;142(1):70-81.
50. Girotra M, Naveiras O, Vannini N. Targeting mitochondria to stimulate hematopoiesis. *Aging (Albany NY)*. 2020;12(2):1042-1043.
51. Filippi MD, Ghaffari S. Mitochondria in the maintenance of hematopoietic stem cells: new perspectives and opportunities. *Blood*. 2019;133(18):1943-1952.
52. Bertaux A, Cabon L, Brunelle-Navas MN, Bouchet S, Nemazanyy I, Susin SA. Mitochondrial OXPHOS influences immune cell fate: lessons from hematopoietic AIF-deficient and NDUFS4-deficient mouse models. *Cell Death Dis*. 2018;9(6):581.
53. Snoeck HW. Mitochondrial regulation of hematopoietic stem cells. *Curr Opin Cell Biol*. 2017;49:91-98.
54. Maryanovich M, Zaltsman Y, Ruggiero A, et al. An MTCH2 pathway repressing mitochondria metabolism regulates haematopoietic stem cell fate. *Nat Commun*. 2015;6:7901.
55. Yu WM, Liu X, Shen J, et al. Metabolic regulation by the mitochondrial phosphatase PTPMT1 is required for hematopoietic stem cell differentiation. *Cell Stem Cell*. 2013;12(1):62-74.
56. Sun X, Cao B, Naval-Sanchez M, et al. Nicotinamide riboside attenuates age-associated metabolic and functional changes in hematopoietic stem cells. *Nat Commun*. 2021;12(1):2665.
57. Wilson BC, Boehme L, Annibali A, et al. Intellectual disability-associated factor Zbtb11 cooperates with NRF-2/GABP to control mitochondrial function. *Nat Commun*. 2020;11(1):5469.
58. Iyer DR, Rhind N. The intra-S checkpoint responses to DNA damage. *Genes*. 2017;8(2):74.
59. Yamane T. Mouse yolk sac hematopoiesis. *Front Cell Dev Biol*. 2018;6:80.
60. Baldarelli RM, Smith CM, Finger JH, et al. The mouse gene expression database (GXD): 2021 update. *Nucleic Acids Res*. 2021;49(D1):D924-D931.
61. McKinney-Freeman S, Cahan P, Li H, et al. The transcriptional landscape of hematopoietic stem cell ontogeny. *Cell Stem Cell*. 2012;11(5):701-714.
62. Bustelo XR, Rubin SD, Suen KL, Carrasco D, Barbacid M. Developmental expression of the vav protooncogene. *Cell Growth Differ*. 1993;4(4):297-308.
63. Huang XF, Nandakumar V, Tumurkhuu G, et al. Mysm1 is required for interferon regulatory factor expression in maintaining HSC quiescence and thymocyte development. *Cell Death Dis*. 2016;7(6):e2260.
64. Shin JY, Hu W, Naramura M, Park CY. High c-Kit expression identifies hematopoietic stem cells with impaired self-renewal and megakaryocytic bias. *J Exp Med*. 2014;211(2):217-231.
65. Grinenko T, Arndt K, Portz M, et al. Clonal expansion capacity defines two consecutive developmental stages of long-term hematopoietic stem cells. *J Exp Med*. 2014;211(2):209-215.
66. Kikushige Y, Yoshimoto G, Miyamoto T, et al. Human Flt3 is expressed at the hematopoietic stem cell and the granulocyte/macrophage progenitor stages to maintain cell survival. *J Immunol*. 2008;180(11):7358-7367.
67. Daver N, Schlenk RF, Russell NH, Levis MJ. Targeting FLT3 mutations in AML: review of current knowledge and evidence. *Leukemia*. 2019;33(2):299-312.
68. Buza-Vidas N, Woll P, Hultquist A, et al. FLT3 expression initiates in fully multipotent mouse hematopoietic progenitor cells. *Blood*. 2011;118(6):1544-1548.